

## Water vapor permeation and antimicrobial properties of sago starch based films formed via microwave irradiation

<sup>1</sup>\*Bajpai, S. K., <sup>2</sup>Navin, C. and <sup>3</sup>Ruchi, L.

<sup>1</sup>Polymer Research Laboratory, Department of Chemistry, Govt. Model Science College (Auton.), Jabalpur (M.P.) – 482001, India

<sup>2</sup>Advanced Materials and Processes Research Institute, (Formerly RRL Bhopal), (CSIR), Bhopal (M.P.) - 462064 India

<sup>3</sup>Department of Applied Chemistry, Gyan Ganga College of Technology, Jabalpur, (M.P.) – 482003, India

**Abstract:** This work describes investigation of water vapor permeation properties of sago starch based edible film, prepared by microwave irradiation. The films were characterized by the FTIR, XRD, DSC and Tensile strength measurements. The equilibrium moisture content (EMC) data, obtained at 23 and 31°C was fairly interpreted in terms of well known GAB isotherm model. The extent of water vapor, permeated through films was observed to increase with temperature and relative humidities of surrounding environments but decrease with thickness of the films. The rate of water vapor permeation showed a linear relationship with thickness of the films. The presence of chitosan micro particles within the films matrix also caused a decrease in the extent of moisture permeated. Finally the films were loaded with ethylenediamine tetra acetic acid (EDTA) as antimicrobial agent. These films showed excellent antibacterial action against *E. coli*.

**Keywords:** Sago starch films, microwave, edible film, GAB isotherm, antimicrobial properties

### Introduction

The development of edible films or coatings based on petrochemicals has now turned towards biodegradable and/or edible films (Tharnathan *et al.*, 2003), mainly because of environmental reasons. Although biodegradable films are more expensive than the petrochemical materials, they will biodegrade into CO<sub>2</sub>, water and biomass under aerobic conditions or methane and biomass under anaerobic conditions (Avella *et al.*, 2005). Based on these characteristics biodegradable films can contribute effectively towards reducing environmental pollution. The materials used are mainly polysaccharides (Bourtoom *et al.*, 2008, Zhong *et al.*, 2008, Boonsong *et al.*, 2009, Silva *et al.*, 2009, Bangyekar *et al.*, 2006, Olivas *et al.*, 2008), proteins (Mateos *et al.*, 2009, Ozdemir *et al.*, 2008, Yoshida *et al.*, 2003, Jia *et al.*, 2009) and lipids, or combination of these components. Indeed, biodegradable polymer films are not meant to totally replace synthetic packaging films, but to limit moisture, aroma and lipid migration between food components where traditional packaging can not function. In other words, biodegradable and edible films can be used for versatile food products to reduce moisture loss, to restrict absorption of oxygen, to lessen lipids migration to improve mechanical handling properties and to provide physical protection (Mali *et al.*, 2006). In addition, they may provide other functional advantages

like being carriers of antimicrobials, antioxidants and other preservatives (Cagri *et al.*, 2001)

Recently, due to growing concern of the consumers regarding the safety of food stuff from pathogen contamination, there has been more emphasis on the development of antimicrobial packaging films that can be employed for controlling the microbiological decay of perishable food products (Nobile *et al.*, 2008, Sivarooban *et al.*, 2008, Moller *et al.*, 2004). Different organic and inorganic active agents can be incorporated into polymeric edible films to prevent the undesirable microbial spoilage occurring during storage of packaged fresh food (Lee *et al.*, 2004).

The use of natural plant extract is desirable for development of new food products and nutraceuticals as well as new active packaging systems. In this connection we hereby propose microwave induced synthesis of ethylenediaminetetraacetic acid loaded sago starch edible films with fair antibacterial properties. Sago starch is isolated from sago palm (*metroxylon* spp.), and has been well distributed throughout South East Asia (Ahmad *et al.*, 1999). According to a published report, sago palms have great potential for starch production (Abd *et al.*, 2002). EDTA is a safe, economical metal chelator which sequesters divalent cations (notably Ca<sup>2+</sup> and Mg<sup>2+</sup>) that contribute to the stability of the outer membrane of Gram-negative bacteria by providing electrostatic interactions with proteins and lipo- polysaccharides (Sivarooban *et al.*, 2008).

\*Corresponding author.

Email: sunil.mnlbpi@gmail.com, polymerlab@rediffmail.com

Furthermore, EDTA releases a large proportion of Gram-negative lipo-polysaccharide from the outer membrane and exposing hydrophobic phospholipids that increases the susceptibility to hydrophobic and cell wall degrading agents (Walsh *et al.*, 2003).

## Materials and Methods

### Materials

Granules of sago starch were received from local merchant and used as received. Other chemicals such as glycerol (GY), ethylenediaminetetraacetic acid (EDTA), and various salts were purchased from High Media Laboratories, Mumbai, India. Nutrient broth and nutrient agar were obtained from Qualigens Fine Chemicals, Mumbai India. The double distilled water was used throughout investigations. Saturated salt solutions of different salts were prepared to provide a wide range of relative humidities (RH) as described elsewhere (Khalloufi *et al.*, 2000).

### Preparation of plain sago starch (PSS) films

PSS film was prepared by microwave induced gelatinization of sago starch followed by evaporation of solvent. In brief, 1 g of sago starch was added into 20 ml of distilled water at 70°C followed by addition of 0.25 ml of glycerol. The total volume of colloidal dispersion, so obtained, was made up to 25 ml by addition of appropriate quantity of water. The colloidal dispersion was put in microwave oven (LG, model MS-1947C) and irradiated at 640 Watt for 30 seconds, which yielded an almost transparent solution. The solution was poured into Petri dish and put in an electric oven (Tempstar, India) at 50°C for a period of 24 hrs. Finally the film was peeled off and kept in a dessicator for further use.

In order to prepare EDTA loaded films, a pre-calculated quantity of EDTA was also added into aqueous solution of sago starch. The films so obtained were designated as EDTALSS (x) films, where the number x in parenthesis denotes the amount of EDTA (in mg) present per gram of starch in the films.

### Film thickness measurements

Thickness of the films was measured with micrometer screwguage (Yaweh company, Africa), at five random locations on the film. Mean thickness value for each sample was calculated and used in water vapor permeability (WVP) calculations.

## Characterization of film

### FTIR – Spectral analysis

The FTIR Spectra of Glycerol plasticized sago

starch film was recorded on Shimadzu 8400 S Fourier Transformation Infrared spectrophotometer using KBr.

### XRD Analysis

XRD analysis was performed with a Miniflex II desktop Xray Diffractometer (Japan).

### DSC Analysis

DSC analysis was performed with a Metter DSC-30 thermal analyzer with sago starch film (with no glycerol) and glycerol plasticized sago starch films. Film of known weight was taken in a sealed aluminium pans and the sample was heated from 40 to 240°C at the heating rate of 10°C per minute under constant flow of argon gas.

### Tensile strength analysis

Tensile strength was measured with a LLOYD instrument (Model LR30K, LLOYD) Instrument Ltd; Hampshire, England) as per ASTM D882-91 standard method. Five samples 2.54 cm x 12 cm were cut from each film. Initial grip separation and cross head speed were set at 50 mm and 50 mm/min respectively. Tensile strength was calculated by dividing the maximum force by the initial specimen cross sectional area.

### SEM Analysis

The morphological features of plain sago starch film and chitosan microparticles loaded plain sago starch film were observed using a JOEL JSM-6390A (Japan) Analytical scanning electron microscope.

### Equilibrium moisture sorption studies

The moisture sorption isotherms were determined gravimetrically using the static method as described by Alhamadan *et al.* (Alhamdan *et al.*, 1999). Constant relative humidity (RH) atmospheres were obtained with saturated salt solutions (CH<sub>3</sub>COOK, K<sub>2</sub>CO<sub>3</sub>, NaBr, NaCl, KCl, BaCl<sub>2</sub> and K<sub>2</sub>SO<sub>4</sub>) covering a water activity range from 0.23 to 0.90 at desired temperature. Triplicate samples of the pre-weighed dried samples were placed inside each of the eight desiccators containing the saturated salt solutions. The samples were weighed periodically (every day for a period of seven days) until the percentage of sample mass, changed between two successive measurements, was less than 1%. The moisture adsorbed by samples was calculated using the following expressions:

$$\text{Equilibrium Moisture Content (EMC)} = \frac{W_e - W_o}{W_o} \quad (\text{g/g film})$$

where  $W_o$  and  $W_e$  are weights of the film in the

initial and equilibrated state respectively.

#### Water vapor permeation studies

Water vapor permeability (WVP) of the films was determined gravimetrically using a modified ASTM E96-00(2000) procedure. The permeation cell (acrylic cups) had an internal diameter (id) of 4.4 cm and an external diameter (ed) of 8.4 cm (exposed area: 15.205 cm<sup>2</sup>). They were 3.5 cm deep and contained CaCl<sub>2</sub> (0% RH;  $OP_a$  water vapor partial pressure). Film was placed between the cell and its acrylic ring shaped cover (4.4 cm id and 8.4 cm ed) which was adjusted to the cup with four screws located describing a cross. A 7 mm air gap was left between the films and the CaCl<sub>2</sub> layer. The pre-weighed covered cell was put in a temperature and RH controlled chamber, maintaining desired RH and temperature. Mass measurements of cups were done at regular time intervals using an electronic balance (Denver, Germany) with the accuracy of 0.0001g. All tests were conducted in triplicate and WVP and other related parameter were calculated using following expressions.

$$\text{Water Vapor transmission rate (WVTR)} = \frac{\Delta W}{\Delta t} \cdot \frac{1}{A} \text{ g s}^{-1} \text{ m}^{-2} \dots (1)$$

$$\text{Permeance (P)} = \frac{\Delta W}{\Delta t} \cdot \frac{1}{A \Delta P} \text{ g s}^{-1} \text{ m}^{-2} \text{ Pa}^{-1} \dots (2)$$

$$\text{Water Vapor Permeability (WVP)} = \frac{\Delta W}{\Delta t} \cdot \frac{\chi}{A \Delta P} \text{ g s}^{-1} \text{ m}^{-1} \text{ Pa}^{-1} \dots (3)$$

where  $\Delta W/\Delta t$  is the amount of water gain per unit time of transfer,  $\chi$  is the film thickness (m), A is the area exposed to the water transfer (m<sup>2</sup>) and  $\Delta P$  is the water vapor difference between both sides of the film. All the experiments were done in triplicate and average values have been reported in the data.

#### Antimicrobial studies

The biocidal action of EDTA loaded films was investigated in qualitative and quantitative manners (Thomas *et al.*, 2007), using *E. coli* as model bacteria. One hundred micro liters of the inoculums solution was added to 20 ml of the appropriate soft agar, which was overlaid on to Petri dishes. Circular disks were cut from the test films and placed on the bacterial lawns. The Petri dishes were incubated for 48 hrs at 37°C in the aerobic incubation chamber. The Petri dishes were visually examined for zones of inhibition around the films disc, and the size of the zone diameter was measured at two cross sectional points and the average was taken as the inhibition zone.

For the liquid culture test, each film was cut

into square (1cm×1cm). Three sample squares were immersed in 20 ml nutrient broth in a 25 ml universal bottle. The medium was inoculated with 200 microlitres of *E.Coli* in its late exponential phase, and then transferred to an orbital shaker and rotated at 37°C with speed of 100 rpm. The culture was sampled periodically during the incubation to obtain microbial growth profiles. The same procedure was repeated for the control plain film. The optical density (O.D) was measured at  $\lambda_{\text{max}} = 610 \text{ nm}$  using a spectrophotometer (Shimadzu 6300, Japan).

## Results and Discussion

#### FT-IR spectral analysis

FT-IR analysis of Glycerol plasticized sago starch film Figure 1 shows peak of OH – group stretching at 3576cm<sup>-1</sup>, absorbance near 2960 cm<sup>-1</sup> and 1485 cm<sup>-1</sup> is due to C-H stretching and bending vibration, absorbance band between 1200 cm<sup>-1</sup> and 1000 cm<sup>-1</sup> is due to C-O stretching.

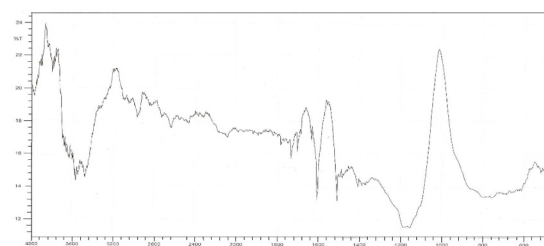


Figure 1. FTIR spectrum of glycerol plasticized sago starch film

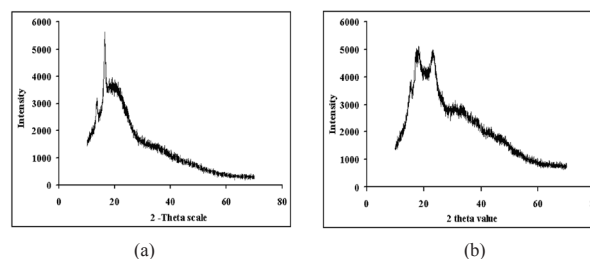
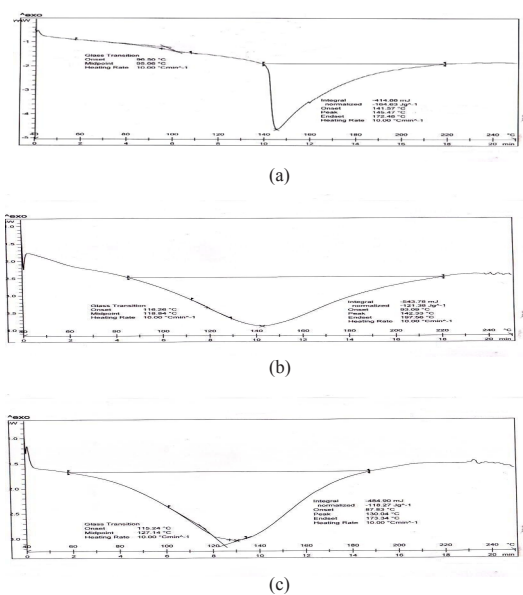


Figure 2(a). X-ray diffraction pattern for (a) Plain Sago starch film and (b) Sago starch powder

#### XRD analysis

The X-ray diffraction patterns of (a) Plain Sago starch film and (b) Sago starch powder have been shown in the Figures 2(a) and (b) respectively. As can be seen, the sago starch powder shows typical A type diffraction pattern with strong reflections at 15.1°, 17°, 17.5° and 23° (Bertuzzi *et al.*, 2007). It also evident that original crystalline structure is slightly modified in the film elaboration process. The film exhibits two reflection peaks, one at 15.1° and the other at 17.2°. An increase in peak intensity and decrease in width indicate enhanced crystallinities in the film. This may be due to fact that starch molecules in the dissolved state, have enhanced chain mobility



**Figure 3.** DSC Thermograms for (a) Sago starch film containing 0wt. % of glycerol (b) Sago starch film containing 20 wt. % of glycerol (c) Sago starch film containing 30 wt. % of glycerol

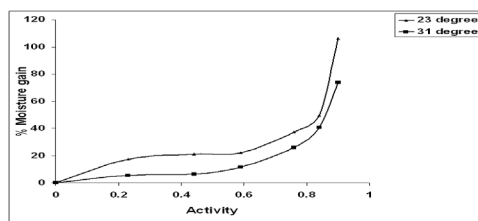


**Figure 4.** GAB Isotherm for plain sago starch film at different temperatures

and this allows possibilities of their rearrangement in networking during film formation process. The amorphous zone, present in both the diffractograms is mainly due to amylopectin (Ahmad *et al.*, 1999).

#### *Effect of plasticizer on crystallinity and tensile strength*

The primary function of adding a plasticizer in the film making is to enhance the film flexibility and reduce brittleness (Yang *et al.*, 2000). At the same time; the crystalline nature of the film is also varied due to addition of plasticizer. The DSC thermo grams of the films plasticized with 0, 20 and 30 wt % of glycerol have been depicted in the Figure 3. It can be observed that the melting temperature, ( $T_m$ ) has slightly shifted to lower values (145.47, 142.3, and 130.04 respectively) and the width of the endothermic peaks became broad with increase glycerol content. The reason is that as a plasticizer with suitable size and three hydroxyl groups, glycerol easily enters into between the film forming polymeric chains and weakens the intermolecular forces between the polymer and decreases the crystallinity. In addition, -OH group of glycerol molecules may also interact

with hydroxyl groups of starch molecules thus making it difficult for starch polymeric chains to re-arrange themselves during storage period (Chen *et al.*, 2008).

We also measured tensile strength (TS) of plasticized films. The film without glycerol was almost brittle. However the film containing 20, 30 and 40 wt % glycerol showed TS values of 5.14, 2.55 and 2.17 MP<sub>a</sub> respectively. The observed decrease may be attributed to the weakening of intermolecular H-bondings between starch molecules due to presence of glycerol molecules in between them.

#### *Equilibrium moisture sorption studies*

The moisture sorption isotherms of plain sago starch film at 23 and 31°C are shown in the Figure 4 it is quite clear that all curves show typical sigmoidal shape, thus confirming type II classification which is characteristic of biological materials, and high molecular weight sugars which absorb relatively small amount of water at lower activity and large amount at higher relatively humidities (Bag *et al.*, 2009). It is also clear that for a given water activity, equilibrium moisture content decreases with increase in temperature. This may be simply explained on the basis of the fact that increase in temperature causes an increase in kinetic energy of water vapor molecules and therefore vander Waals forces of attraction between sorbed water molecules and starch films becomes weak, thus causing a decrease in moisture uptake. Therefore moisture sorption may be regarded as exothermic process. Similar results have been reported elsewhere (Sinija *et al.*, 2008).

Several isotherm models have been proposed for the correlation of the equilibrium moisture content with the water activity ( $a_w$ ) of food products. Among the most efficient equations for the prediction of the experimental data, the well known GAB isotherm model can be mentioned (Clement *et al.*, 2008). The major advantages of the GAB model are its viable theoretical background, need for only three parameters (with physical meaning) and its capacity to describe the sorption of water vapor in foods up to water activity of 0.9 by just multiplying the activity by a constant less than unity (Lomauro *et al.*, 1985) The GAB equation is normally written in the following form:

$$M_c = \frac{M_0 C K a_w}{(1 - K a_w)(1 - K a_w + C K a_w)} \quad \dots (4)$$

where  $M_c$  is the moisture content of the material on a dry basis (g/g dry basis),  $C$  is the Guggenheim constant related to heat of sorption,  $a_w$  is water activity,  $K$  is the constant related to multilayer molecules properties and  $M_0$  is the moisture content

of monolayer in BET theory.

After transformation, GAB equation has an equivalent form to the Hailwood and Horrobin (1946) equation (Hailwood *et al.*, 1946)

$$\frac{a_w}{M_c} = (b_3 a_w^2 + b_2 a_w + b_1) \dots (5)$$

From the parameters  $b_1$ ,  $b_2$  and  $b_3$ , the values of constants  $K$ ,  $C$  and  $M_0$  were calculated through following relations

$$K = \frac{-\beta \pm \sqrt{\beta^2 - 4\alpha\lambda}}{2\lambda} \dots (6)$$

$$C = \frac{2 \pm (\sqrt{\beta^2 - 4\alpha\lambda})}{-\beta + \sqrt{\beta^2 - 4\alpha\lambda}} \dots (7)$$

$$M_0 = \frac{1}{\sqrt{\beta^2 - 4\alpha\lambda}} \dots (8)$$

The moisture content data were transformed by dividing the water activity ( $a_w$ ) with equilibrium moisture content ( $M_0$ ). A quadratic curve of polynomial function was obtained from these data points. The values of  $b_1$ ,  $b_2$  and  $b_3$  obtained using nonlinear regression analysis of the experimental data were used to obtain GAB constants  $M_0$ ,  $C$  and  $K$ . The isotherm constants, related with GAB model, were evaluated using equations (6), (7) and (8) and are given in the Table I. Out of the three constants namely  $M_0$ ,  $K$  and  $C$ , the monolayer moisture content  $M_0$  is of particular interest because it indicates the amount of water that is strongly adsorbed to specific sites of the film surface. It is clear from the data given that moisture content  $M_0$  decreases with the increases in temperature. Similar results have also been reported in our previous studies on the chitosan based edible films (Bajpai *et al.*, 2009).

**Table I.** Parameter for GAB isotherm model, obtained using equilibrium moisture uptake data at different temperatures

Parameters	Temperatures (°C)	
	23	31
C	8.7333	162.762
K	0.9956	1.0729
$M_0$	0.0893	0.0393

*Water vapor permeability studies*

Watervaporpermeability(WVP)isproportionality constant and is assumed to be independent of water vapor gradient across the film. However, when the films are made from polysaccharides and protein, they contain hydrophilic polar groups that interact with water molecules, thus causing deviation

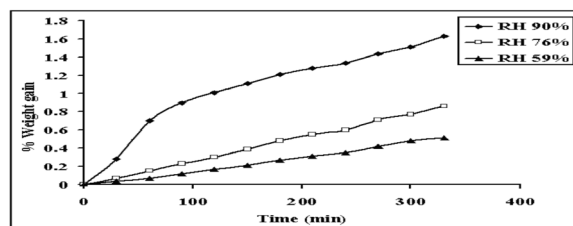


**Figure 5.** Kinetics of Water vapor permeation through PSS film at different RH and same temperature (28°C)

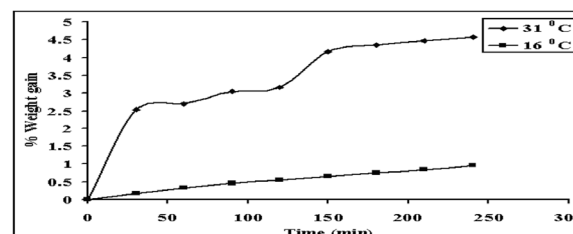


**Figure 6.** Kinetics of Water vapor permeation through PSS film at different temperature and same RH (100%)

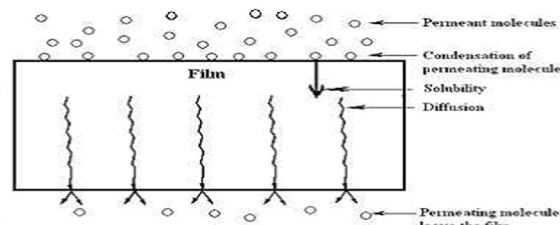


**Figure 7.** Scheme showing permeation of water vapor through a film

(Moreira *et al.*, 2003). Since edible films are intended to be made to impede moisture transfer between food and surrounding atmosphere, WVP is a significant parameter and must be studied.

The results of water vapor permeation experiments, carried out at three relative humidities, namely 59, 76 and 90 percent at 28°C, have been shown in Figure 5. It is clear that amount of vapors permeated through the films increases with relative humidity. The WVTR, obtained using the kinetics moisture permeation data, were found to be  $3.10 \times 10^{-4}$ ,  $5.38 \times 10^{-4}$  and  $11.8 \times 10^{-4} \text{ gs}^{-1}\text{m}^{-2}$  respectively for the relative humidities of 59, 76 and 90 percent. Clearly the permeability increases with relative humidity of the environment. This may be simply being attributed to the fact that difference in vapor pressure across the film acts as a driving force for their permeation.

The dynamic permeation of water vapors through PSS films at two different temperatures namely 16 and 31°C has been shown in the Figure 6. The almost linear plots permit the determination of WVTR. It is evident that permeation of water vapor through films is enhanced with the increase in temperature. The observed findings may be explained on the basis of the mechanism through which water vapor molecules are believed to permeate through films. As shown in Figure 7, permeation of water vapor through film occurs in following steps: (i) condensation

of permeating molecules on the surface (ii) their solubilization (iii) their diffusion across the width of the film and (iv) their departure from the other side of the films. All these steps have been shown in the Figure 7. In the light of this mechanism, the observed increase in water vapor transmission with temperature may be explained as follows: when temperature is raised, except the first step i.e. condensation of water vapor molecules on the surface, all remaining steps are enhanced. In the other words, their solubilization, diffusion across the film and desorption at other side undergo appreciable enhancement. Hence the overall effect is the enhancement in the water vapor permeability with temperature. The various permeation parameters calculated using equations (1), (2) and (3) have been given in Table II (a) and (b). The values of different parameters obtained also support observed findings.

**Table II(a).** Various parameters obtained for permeation of water vapors through PSS film at different relative humidities at 28°C

Parameters	Relative humidity of environment (%)		
	59	76	90
WVTR ( $gs^{-1}m^{-2}$ )	$3.10 \times 10^{-4}$	$5.38 \times 10^{-4}$	$11.81 \times 10^{-4}$
Permeance ( $gs^{-1}m^{-2}Pa^{-1}$ )	$8.39 \times 10^{-8}$	$1.13 \times 10^{-7}$	$2.09 \times 10^{-7}$
Permeability ( $gs^{-1}m^{-1}Pa^{-1}$ )	$1.93 \times 10^{-11}$	$2.59 \times 10^{-11}$	$4.8 \times 10^{-11}$

**Table II(b).** Various parameters obtained for water vapor permeation through PSS film at different temperature at 100 percent relative humidity

Parameter	Temperatures (°C)	
	31	16
WVTR ( $gs^{-1}m^{-2}$ )	$48.9 \times 10^{-4}$	$8.705 \times 10^{-4}$
Permeance ( $gs^{-1}m^{-2}Pa^{-1}$ )	$7.796 \times 10^{-7}$	$1.387 \times 10^{-7}$
Permeability ( $gs^{-1}m^{-1}Pa^{-1}$ )	$17.91 \times 10^{-11}$	$3.19 \times 10^{-11}$

#### Effect of presence of chitosan on permeability

Although sago starch is a biodegradable polymer, but its hydrophilic nature causes a loss of barrier properties thus preventing its industrial applications. Permeability in the films is controlled by diffusivity and solubility of water within the film matrix. The addition of surfactants to the edible films has been a successful way to impede the permeation of water vapors through the films (Villalobos *et al.*, 2006). Using nano science new forms of tightly linked three dimensional networks can be developed to prevent migration of water in food products. In the work described by Lotti *et al.* (2008) it was observed that nano composite films (HDPE + organophilic treated clay) had a significant decrease of barrier properties (water and  $O_2$  permeability) in comparison to pure

HDPE films. The trend was attributed to the formation of water clusters. The effectiveness of the reinforcing effect of nanosize microcrystalline cellulose fillers in HPMC film has also been reported by Dogan and McHug (Dogan *et al.*, 2007). In the present work tripolyphosphate (TPP)- cross linked chitosan microparticles were introduced into plain sago starch films and their water permeation properties were investigated at 100 percent RH at 28°C. The results, as shown in the Figure 8, clearly reveal that plain film shows greater vapor permeability as compared to the films which contain 100, 150 and 200 mg of chitosan microparticles per gram of sago starch. In addition the permeability decreases to a greater extent with increase in chitosan content. The observed decrease could be attributed to the formation of intermolecular hydrogen bonding between  $NH_3^+$  groups of the chitosan and  $-OH$  of the starch. The amino groups ( $NH_2$ ) of chitosan are protonated to  $-NH_3^+$  in acetic acid solution, whereas the ordered crystalline structures of starch molecules were destroyed with microwave-induced gelatinization process, resulting in formation of  $-OH$  group being exposed readily to form hydrogen bonds with  $-NH_3^+$  groups of chitosan (Bourtoom *et al.*, 2008). The compactness in the film structure increased with amount of chitosan, thus enhancing the decrease in permeation of water vapor. The surface morphology of microparticles-loaded film was investigated by scanning electron microscopy (SEM) analysis. Figures 9(a) and 9(b) show the SEM images of surface of plain and chitosan micro particles loaded films respectively. It can be seen that distribution of chitosan particles is almost uniform with the majority of the particles lying in the range of 0.4 to 0.8  $\mu m$ .

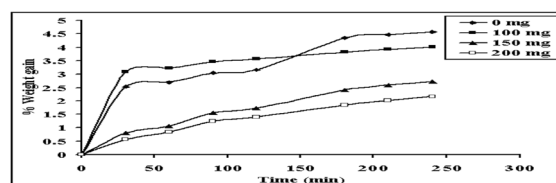


**Figure 8.** Effect of chitosan content on permeability of water vapor through film under relative humidity of 100 %, at 28°C

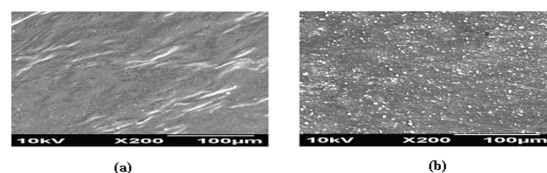


**Figure 9.** SEM images for (a) Plain sago starch film (b) Chitosan microparticles loaded sago starch film

#### Effect of film thickness on permeation

In ideal polymeric structures, gas and vapor permeabilities are independent of the film thickness. However in most of the cases deviations from ideal

behavior have been reported (Park *et al.*, 1995). In the present study, film of varying thickness, in the range of 0.23 to 0.38 mm was prepared and the dynamic permeation of the water vapor was studied under constant relative humidity of 100 percent at 27°C. It is clear from the data, displayed in the Figure 10 that amount of vapor permeated through films decreases with increase in thickness of the films.

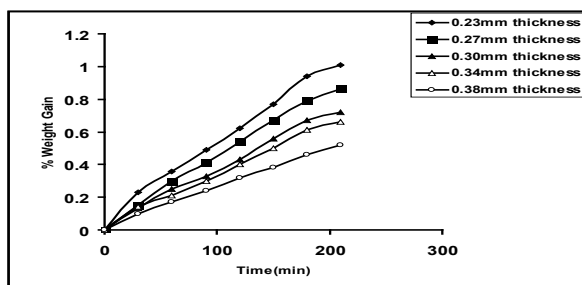


Figure 10. Effect of thickness on permeation of water vapor through films

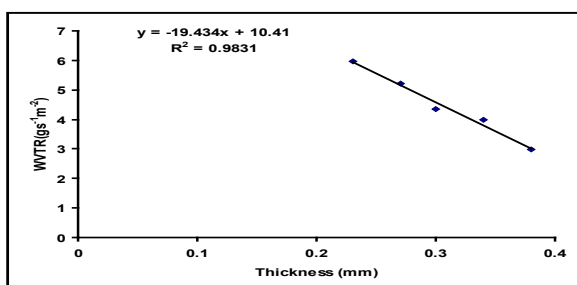


Figure 11. Plot between WVTR and thicknesses of films

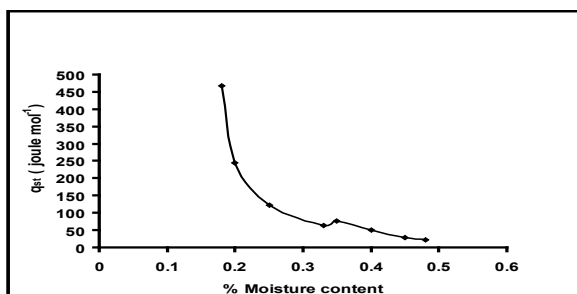


Figure 12. Variation in  $q_{st}$  values with moisture content

This may probably be attributed to the fact that with the increase in thickness water vapor have to travel a greater distance through the film to reach the other side of the film. In the addition, due to hydrophilic nature of the film material, i.e starch, more and more water molecules get attached to the polar groups within the film matrix as the thickness of the films increases. This finally causes a decreases in amount of water vapor that permeate through the films. It is also to be noted here that as the film thickness increases, the film provides an increased resistance to mass transfer across it (Mc Hugh *et al.*, 1993). Finally WVTR, as calculated using equation (1) were plotted against thickness of the film, as shown in the Figure 11. It is clear that there is fair linear relationship between the two as indicated by a fairly

higher regression value of 0.98.

#### Isosteric heat of sorption ( $q_{st}$ )

The net isosteric heat of sorption,  $q_{st}$  also known as binding energy of sorption, is a good measure of interaction of water vapor molecules with solid substrate (Moreira *et al.*, 2003) It may also be considered as indicative of inter molecular attractive forces between the sorption sites and water vapor molecules. The isosteric heat of sorption,  $q_{st}$  was determined using Clausius- Clapeyron equation, given

$$\ln a_w = -\frac{q_{st}}{RT} + I \quad \dots (9)$$

where  $q_{st}$  is the net isosteric heat of sorption ( $J \text{ mol}^{-1}$ ), R is gas constant and I is a integration constant. If  $a_1$  and  $a_2$  are the water activities corresponding to temperatures  $T_1$  and  $T_2$  for a given equilibrium moisture content, then the above equation may be written as

$$\ln \frac{a_2}{a_1} = \frac{q_{st}}{R} \left[ \frac{1}{T_1} - \frac{1}{T_2} \right] \quad \dots (10)$$

Above can be used to determine the isosteric heat of sorption,  $q_{st}$  for given moisture content. The equilibrium moisture uptake data, displayed in Fig. 4 was used to evaluate water activities at two temperature for a given equilibrium moisture content. The  $q_{st}$  values, obtained using equation (10), for different equilibrium moisture contents have been plotted against corresponding moisture contents as shown in Figure 12. The positive values of  $q_{st}$  are indicative of easy physical sorption of water molecules forming a mono layer. A close look at the Figure 12, reveals some interesting facts. The  $q_{st}$  values decrease asymptotically with moisture content which may simply be attributed to the fact that initially sorption occurs on the most active available sites, thus giving rise to high interaction energy. As soon as these sites become occupied, sorption occurs on the less active site and results in less heat of sorption. It is also noteworthy that at low moisture contents, the heat of sorption values are appreciably higher which may probably be due to strong interactions between water vapor molecules and hydrophilic -OH group of sago starch. Similar type of behavior has also been reported elsewhere (Oliveria *et al.*, 2009).

#### Antimicrobial studies

EDTA-incorporated sago starch films were investigated for their anti microbial efficacy against *E.Coli* as model bacteria, by qualitative (zone inhibition method) and quantitative (cell count

method) approaches described in experimental section. In zone-inhibition method different EDTA-loaded films, namely EDTALSS (20 mg), EDTALSS (60 mg), EDTALSS (100 mg) and EDTALSS (150 mg) containing 20, 60, 100 and 150 mg of EDTA were cut in the form of circular disc and investigated for zone inhibition. The PSS film (0 mg EDTA) was used as control. The results as shown in Fig. 13, indicate that Petri dish, supplemented with plain sago starch film (Figure 13) shows dense colonies of bacterial cells throughout while the Petri dishes supplemented with films EDTALSS (20 mg), EDTALSS (60 mg), EDTALSS (100 mg) and EDTALSS (150 mg), demonstrate inhibition action of these films, as is obvious by appearance of circular inhibition zones around the films. A close look at the Fig. 13 reveals that size of the zone increases with amount of EDTA present in the film matrix. The average diameter of circular inhibition zones, obtained by transverse and longitudinal measurements, was found to be 9 mm respectively. The biocidal action of EDTA may simply be attributed to its strong chelating tendency with divalent cations  $\text{Ca}^{2+}$  and  $\text{Mg}^{2+}$  ions that contribute to the stability of the outer bacterial membrane by providing electrostatic interactions with proteins and lipo-polysaccharides (Sivarooban *et al.*, 2008). Finally, the kinetics of bacterial killing was also investigated (Figure 14). It is evident that there is an appreciable growth rate of bacteria in the control set while the growth rate is suppressed appreciably in the solution containing the pieces of film EDTALSS (60 mg). Both of the above experiments establish the fair inhibitory actions of these films.

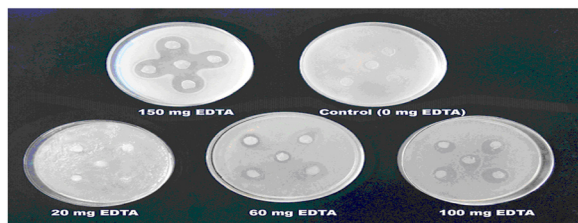


**Figure 13.** Evaluation of antibacterial action for (A) EDTALSS (20 mg) (B) EDTALSS (60mg) (C) EDTALSS (100 mg) (D) EDTALSS (150mg) and (E) PSS (0mg) films by zone inhibition method

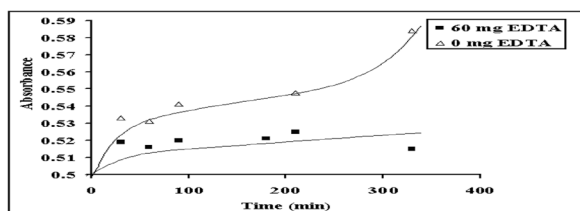


**Figure 14.** Kinetics of bacterial growth for PSS (0mg) and EDTALSS (60mg)

## Conclusion

From the above study it may be concluded that the water vapor permeation properties of sago starch

based edible films, prepared via microwave irradiation, are greatly influenced by temperature, relative humidity, presence of chitosan microparticles. These films exhibit potential to be used as antimicrobial packagings to protect food stuff from microbial infections.

## Acknowledgement

The authors are thankful to Dr. O. P. Sharma, Head, Department of Chemistry for his kind and unconditional support.

## References

- Abd-Aziz, S. 2002. Sago starch and its utilisation. *Journal of Bioscience and Bioengineering* 94(6): 526-529
- Ahmad, F.A., Williams, P.A., Doublier, J., Durand, S. and Buleon, A. 1999. Physico-chemical characterization of sago starch. *Carbohydrate Polymer* 38: 361-370.
- Alhmdan, A.M. and Hasan, B.H. 1999. Water sorption isotherm of Date Pasres as influenced by Date cultivar and storage temperature. *Journal of Food Engineering* 39: 301-306.
- Avella, M., Vliger, J.J De., Errico, M.E., Fischer, S., Vacca, P. and Volpe, M.G. 2005. *Food Chemistry* 93:467.
- Bag, S.K., Srivastav, P.P. and Mishra, H.N. 2009. Desorption and adsorption characteristics of bael (*Aegle marmelos*) pulp and powder. *International Food Research Journal* 16: 561-569.
- Bajpai, S.K., Chand, N. and Chourasiya, V. 2009. Investigation of water vapour permeability and antimicrobial property of zinc oxide nanoparticles-loaded chitosan-based edible films. *Journal of Applied Polymer Science* 115(2): 674-683.
- Bangyekar, C., Aht- Ong, D. and Srikulkit, K. 2006. Preparation and properties evaluation of chitosan-coated cassava starch films. *Carbohydrate Polymer* 63: 61-71.
- Bertuzzi, M. A., Vidaurre Castro E.F., Armada, M. and Gottifredi, J.C. 2007. Water vapor permeability of edible starch based films. *Journal of Food Engineering* 82: 972-978.
- Boonsong, P., Laohakunjit, N.N., Kerdchoechuen, O. and Tusvil, P. 2009. Properties and permeability of aroma compounds in food through plasticized cassava films. *International Food Research Journal* 16: 97-103.
- Bourtoom, T. and Chinnan, M.S. 2008. Preparation and properties of rice starch- chitosan blend biodegradable

- film. *LWT-Food Science and Technology* 41: 1633-1641.
- Cagri, A., Ustunol, Z. and Ryser, E.T. 2001. Antimicrobial edible films and coatings. *Journal of Food Science* 66(6): 865-84.
- Chen, J., Liu, C., Chen, Y., Chan, Y. and Chang, P.R. 2008. Structural characterization and properties of starch/konjac glucomannan blend films. *Carbohydrate Polymer* 74: 946-952.
- Clement, Y. B.Y., and Tano, K. 2008. Experimental determination of the Sorption isotherms of "Beta" Lactose, New Water Absorbent and Sodium Bicarbonate *Journal of Food Technology* 6(4): 152-157.
- Da Silva, M.A., Bierhalz, A.C.K. and Kieckbusch, T.G. 2009. Alginate and pectin composite films crosslinked with  $Ca^{2+}$  ions: Effect of the plasticizer concentration. *Carbohydrate Polymer* 77: 736-742.
- Dogan, N. and Mc Hugh, T.M. 2007. Effect of microcrystalline cellulose on functional properties of hydroxypropylmethylcellulose microcomposite films. *Journal of Food Science* 72(1): 16-22.
- Hailwood, A.J. and Horrobin, S. 1946. Adsorption of water by polymer: Analysis in terms of a simple model. *Transaction Far. Society* 42: 84-92.
- Jia, D., Fang, Y. and Yao, K. 2009. Water vapour barrier and mechanical properties of konjac glucomannan-chitosan-soyprotein isolate edible films. *Food and Bioproducts Processing* 87: 7-10.
- Khalloufi, S., Giasson, J. and Ratti, C. 2000. Water activity of freeze dried mushrooms and berries. *Canadian Agricultural Engineering* 42(1): 7.1-7.13.
- Lee, C.H., An, D.S., Park, H.J. and Lee, D.S. 2004. A coating for use as an antimicrobial and antioxidants packaging materials incorporating nisin and  $\alpha$ -tocopherol. *Journal of Food Engineering* 62: 323-329.
- Lomauro, C.J., Bakshi, A.S. and Labuza, T.P. 1985. Evaluation of food moisture isotherm equations. Part I; Fruit, vegetables and meat products. *International Journal of Food Science and Technology* 18: 111-117.
- Lotti, C., Isaac, C.S., Branciforti, M.C., Alves, R.M.V., Liberman, S. and Bretas, R.E.S. 2008. Rheological, mechanical and transport properties of blown films of high density polyethylene nanocomposites. *European Polymer Journal* 44(5): 1346-1357.
- Mali, S., Grossmann, M.V.E., Garcia, M.A., Martino, M.N. and Zaritzky, N.E. 2006. Effect of controlled storage on thermal, mechanical and barrier properties of plasticized films from different starch sources. *Journal of Food Engineering* 75: 453-460.
- Mateos, M.P., Montero, P. and Gomez-Guillen, M.C. 2009. Formulation and stability of biodegradable films made from codgelatin and sunflower oil blends. *Food Hydrocolloids* 23: 53-61.
- Mc Hugh, T.H., Bustillos-Avena, R. and Krochta, J.M. 1993. Hydrophilic edible films: modified procedure for water vapor permeability and explanation of thickness effects. *Journal of Food Science* 58(4): 899-903.
- Moller, H., Grelier, S., Pardon, P. and Coma, V. 2004. Antimicrobial and physicochemical properties of chitosan-HPMC based films. *Journal of Agricultural and Food Chemistry* 52: 6585-6591.
- Moreira, R., Vazquez, G., Chenlo, F. and Carballal, J. 2003. Desorption isotherms of *Eucalyptus globulus* modelling using G.A.B. equation. *EJEA Chemistry* 2 (3): 351-355.
- Nobile, M.A.D., Conte, A., Incoronato, A.L. and Panza, O. 2008. Antimicrobial efficacy and release kinetics of thymol from zein films. *Journal of Food Engineering* 89: 57-63.
- Olivas, G.I. and Barbosa-Canovas G.V. 2008. Alginate-calcium films: water vapour permeability and mechanical properties as affected by plasticizer and relative humidity. *LWT- Food Science and Technology* 41: 359-366.
- Oliveira, E.G., Rosa, G.S., Moraes, M.A. and Pinto, L.A.A. 2009. Moisture Sorption Characteristics of Microalgae *Spirulina Plantensis*. *Brazilian Journal of Chemical Engineering* 26(01): 189-197.
- Ozdemir, M. and Floros, J.D. 2008. Optimization of edible wey protein films containing preservatives for water vapour permeability, water solubility and sensory characteristics. *Journal of Food Engineering* 86: 215-224.
- Park, H.J. and Chinnan, M.S. 1995. Gas and Water vapor barrier properties of edible films from protein and cellulosic materials. *Journal of Food Engineering* 25: 497-507.
- Sinija, V.R. and Mishra, H.N. 2008. Moisture sorption isotherms and heat of sorption of instant (soluble) green tea powder and green tea granules. *Journal of Food Engineering* 86: 494-500.
- Sivaroban, T., Hettiarachchy, N.S. and Johnson, M.G. 2008. Physical and antimicrobial properties of grape seed extract, nisin and EDTA incorporated soy protein

edible films. *Food Research International* 41: 781-785.

Tharanathan, R.N. 2003. Biodegradable films and composite coatings. Past, present and future Trends in *Food Sci. Technology* 14: 71-78.

Thomas, V., Yallapu, Murli Mohan., Sreedhar, B. and Bajpai, S.K. 2007. A versatile strategy to fabricate hydrogel-silver nanocomposites and investigation of their antimicrobial activity. *Journal of Colloid and Interface* 315: 389 -395.

Villalobos, R., Hernandez –Munoz, P. and Chiralt, A. 2006. Effect of surfactants on water sorption and barrier properties of hydroxypropylmethyl cellulose films. *Food Hydrocolloids* 20(4): 502-509.

Walsh, S.E., Maillard, J.Y., Russell, A.D., Catrenich, C.E., Charbonneau, D.L. and Bartolo, R.G. 2003. Activity and mechanism of action of selected biocidal agents on gram-positive and gram –negative bacteria. *Journal of Applied Microbiology* 94: 240-247.

Yang, L. and Paulson, A.T. 2000. Mechanical and water vapor barrier properties of edible gaellan films. *Food Research International* 33:563-570.

Yoshida, C.M.P., Antunes, A.C.B., Antunes L.J. and Antunes, A.J. 2003. *International Journal Food Science Technology* 38: 595-601.

Zhong, Q. and Xia, W. 2008. Physicochemical properties of edible and preservative films from chitosan/cassava starch/gelatin blend plasticized with glycerol. *Food Technology and Biotechnology* 46(3): 262-269.